A. Saint-Jalmes , S. Marze, M. Safouane and D. Langevin*

Foam Experiments in Parabolic Flights: Development of an ISS Facility and Capillary Drainage Experiments

We report results of experiments on aqueous foams performed under microgravity conditions obtained during parabolic flights. After a presentation of the FOAM project for the International Space Station (concepts, objectives and technical issues), we show how some of the technical issues can be addressed in parabolic flights. Results on different methods of controlled foam production, and on prototype rheological cells are presented, also offering us the opportunity to review and describe methods of foam production. On the scientific side, we present results of different types of capillary drainage (or imbibition) experiments, based on light scattering measurements. These experiments, performed for the first time on 3D foams with controlled bubble size, surface chemistry and liquid injection rates, are in good agreement with the theoretical predictions.

Authors:

A. Saint-Jalmes, S. Marze, M. Safouane and D. Langevin
Laboratoire de Physique des Solides
Université Paris-Sud, 91405 Orsay, France.

* Author for correspondence:
saint-jalmes@lps.u-psud.fr

Paper submitted: XX.YY.ZZZZ
Submission of final revised Version: XX.YY.ZZZZ
Paper finally accepted: XX.YY.ZZZZ

1. Introduction

Aqueous foams - dispersions of a gas into a liquid containing surfactant molecules - are common in our everyday life: in cosmetics, food products, detergency, light-weight materials. They are also important in many industrial processes (flotation, oil recovery, firefighting, paper…) [1-3]. Indeed, aqueous foams have very intriguing properties: for instance, though made simply of gas and liquid, one can hold them in hands, where they behave like solids (think about shaving cream, or chocolate mousse...). The solid character is related to the fact that the foam bubbles are tightly packed, deformed and jammed, so that they cannot move by themselves. As for many other foam properties, the mechanical behavior strongly depends on the amount of compaction of the gas bubbles, and thus in the amount of liquid inside the foam (characterized by the foam liquid fraction $\varepsilon = V_{liquid}/ V_{foam}$) [1-3]. Elucidating completely the physics of foams requires to know and to understand the properties of foams at any liquid fractions (from the very "dry" to the very "wet" limit).

However, the study of wet foams remains almost impossible on ground due to gravity effects (gravitational drainage): as liquid and gas naturally separate, the liquid initially distributed inside the foam flows downward through it, and leaks out at the bottom, thus always transforming a wet foam into a dry one [1-6]. Moreover, experiments show that the higher the initial liquid fraction, the faster the drainage, so that wet foams evolve extremely fast on Earth. Beside drainage, other effects naturally occur in foams: coarsening due to gas diffusion between bubbles, bubble coalescence, or film rupturing. Due to all these effects, a foam irreversibly evolves with time (it "ages"), and understanding this aging is crucial for all the applications. On ground, the difficulty to understand these different processes, which all depend on the foam liquid fraction, resides in the fact that they are all coupled via the gravitational drainage, which irreversibly modifies this liquid fraction with time, making the analysis of ground measurements rather complicated.

Only microgravity conditions offer the opportunity to study the properties of wet foams, meaning that it can allow us to study foams at any constant and homogeneous liquid fractions

over long periods of time. In this context, the "FOAM" experimental module for the Microgravity Science Glovebox (MSG) of the International Space Station (ISS) is now developed, under the supervision of ESA. This project associates the authors research group in France, the one of D. Weaire from the Trinity College in Dublin (Ireland), the ones of M. Adler and R. Hohler in the Marne-la-Vallée university (France) and the one of D.J. Durian at University of Pennsylvania (USA).

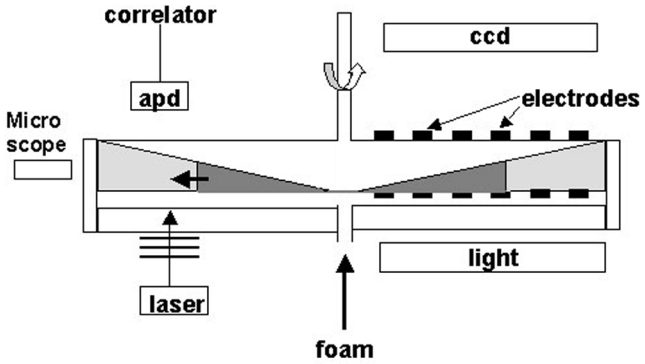

Fig. 1 : Experimental concept of the FOAM module for the ISS, showing the rheometer cell geometry, and the different optical and electrical diagnostics.

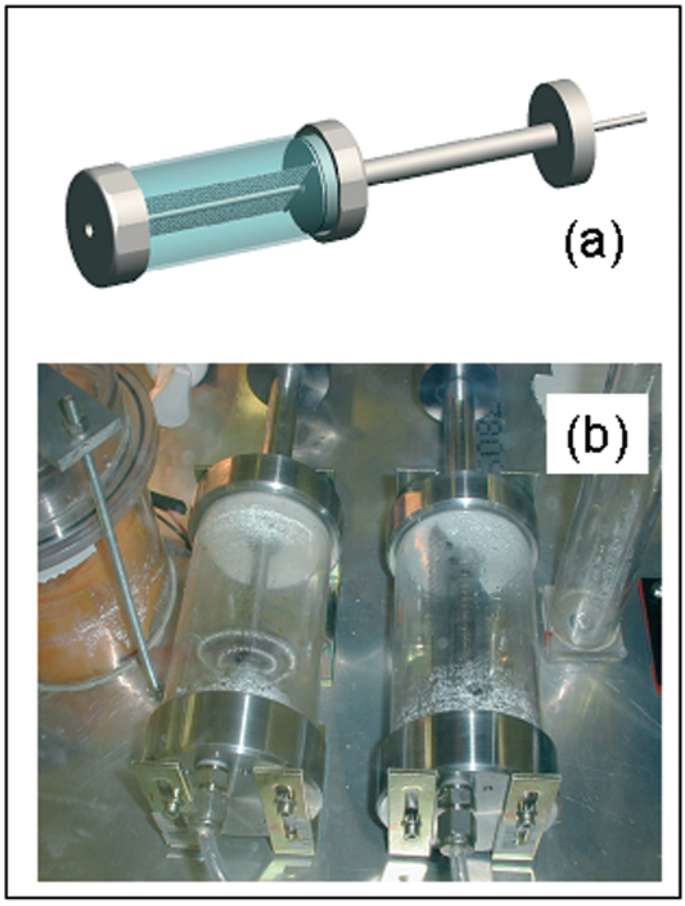

Fig. 2 : Mechanical mixers for foam production. (a) drawing of the mixer with the rotating mesh, and (b) picture of two of these mixers (on the right, same as in (a)).

In this paper after describing the goals and main concepts of the FOAM module (section 2) needed for explaining the aims of the parabolic flight tests, we present the results obtained during such flights (technical tests in section 3, and imbibition results in section 4).

2. The ISS foam module: concepts and goals

The scientific studies to be performed in the FOAM module deal with: the mechanical (rheological) properties of aqueous wet foams, capillarity-induced liquid imbibition in foams, foam coarsening processes, and the physicochemical origins of foam stability. On all these issues, new results can be expected as all the complex coupling with gravitational drainage will be removed. It is foreseen to develop a single cell for the rheological, imbibition and coarsening experiments (representing mostly all the physics-oriented issues). The most stringent requirements for the design of such a cell are imposed by the rheometry needs [7]. The cell containing the foam will have a flat cylindrical shape, with an inside "cone-plate" geometry in order to apply controlled and homogeneous shears on the samples [1-3,7]: the top part of the cell has a conical shape, and is able to rotate on its axis, while the bottom plate part is fixed (Fig. 1). The whole cell has to be transparent for optical purposes (though some roughness is needed at the inside surfaces to avoid slippage of the sample). The typical 3 dimensions of such a cell are a diameter of 15 cm and a cone angle of 0.2 rad, resulting in cell thickness at the edge of 1.5 cm. Rheometry employs torque measurements on the axis, when oscillatory or continuous rotation (shear) are imposed. The foam is injected in the cell through the bottom at the center. It is also at this location that some surfactant solution (the same as the one used to make the foam) can be injected into the foam at controlled flow rates for the imbibition experiments. In fig. 1, the foam appears in grey, confined between the cone and the plate. The darker grey represents a wetter foam, obtained as some liquid is injected during an imbibition experiment. To measure and follow the foam liquid fraction profile, a set of electrodes is inserted along a radius on both side of the cell ; the electrical conductivity being proportional to the liquid fraction [1-3]. Optical diagnostics are also foreseen using either a highly coherent laser light or an extended white light. With the laser on one side of the cell, associated with an avalanche photodiode (APD) and a correlator on the other, Diffusive Wave Spectroscopy (DWS) can be performed in order to measure photon correlation functions, and to investigate the dynamics at the bubble scale under shear [8]. The white light source, associated to a CCD camera, is dedicated to follow the foam behavior inside the cell during filling, cleaning, etc…. A microscope also allow us to visualize a few bubbles on the side of the cell. With these coupled methods, one can expect to understand, for instance, what are the features of the "jamming transition" which transforms, as the gas fraction is increased, a viscous bubbly liquid into an elastic foam. Such studies of wet foams can also shed light on universal features

shared by the other "jammed" systems, like emulsions, glasses or granular materials, finally allowing us to clarify the links between the properties at the different length scales. The capillary imbibition and coarsening studies are useful for understanding the structure of wet foams, in order to tests and challenge the theoretical predictions and our understanding of how foams are built when their liquid content is high.

The study of foam stability under microgravity relates more to the physicochemical aspects of foam research. The ultimate goal here is to elucidate the microscopic origins of foamability and stability, by testing different types of foaming agents at different concentrations. In that spirit, different small and parallelepipedic transparent cells will be used. The results obtained should help us for a better understanding of ground behavior, especially regarding the optimization of industrial processes (for instance by understanding how the amount of chemicals or surfactants could be optimized and reduced, in regard of ecological issues). Finally, the knowledge of how to create and control foams in space is important, as they can be used as low-weight/large-volume materials for in-space materials fabrication, as a way of filling any volumes with basically only gas but with a resulting solid structure. In that sense, note that solid foams (polymeric or metallic) are usually made out from the liquid phase of the components, and are thus liquid-like at their origins.

Beside the classical technical issues when developing a microgravity facility (safety, mass, volume, electronics, commands, etc..), some specific ones arise from the nature of an aqueous foam. As a first problem, the foam samples have to be made inside the module, as they cannot be prepared previously on ground. In order to achieve the rheological measurements, the foam bubble size must be of the order of 100μm, and the liquid fraction must be varied from 0.05 to about 0.45. The foam homogeneity and uniformity also have to be very good. With these controlled foams, one has to correctly and uniformly fill the rheological cell (with no voids or holes), then empty it after the measurements, to study a new sample. Such a typical sequence has to be completely reproducible and automatic. In relation with these previous points, one has to optimize the management of the fluids (liquids and gas) so that they can be as much as possible reused for many foams (avoiding large waste reservoirs). There are also issues on the cell itself, which should not leak, though in the same time, it is crucial that there should be no contacts at the periphery of the cone between this rotating piece and the fixed housing (all the friction must come from the foam) (Fig. 1). The treatment of the inner cell surfaces in contact with the foam is also important and has to be optimized, as a compromise between roughness, transparency and wetting properties. Concerning the stability cells, there are similar problems to solve on foam formation and automatic cleaning.

Parabolic flights offer the possibility of conducting experiments in the environment of reduced gravity. We thus participated to the 34th, 35th and 37th ESA parabolic flight campaigns, held in Bordeaux in April 2003, October 2003, and June 2004, where some of the technical issues described above have been explored, as well as the first imbibition experiments in 3D foams.

3. Technical Tests

With the help of the industrial contractors from EADS-ST in Friedrichshafen, we have developed a parabolic flight rack, used in our three campaigns. The core facility consists of three compartments. The bottom and top compartment provides room for power supplies, liquid pump, control and electronics whereas the main compartment in the middle houses the foam experiments (foam generation devices, observation cells and imbibition experiments). Nitrogen was used to create the foams, and a gas bottle was attached on the side floor of the facility. A liquid tank for the surfactant solution, able to hold up to 15 L of surfactant solution, was also attached on the side of the rack. During the flight campaigns, solutions of a cationic surfactant, tetradecyltrimethylammonium bromide (TTAB), were used. The choice of this surfactant was made in relation with long

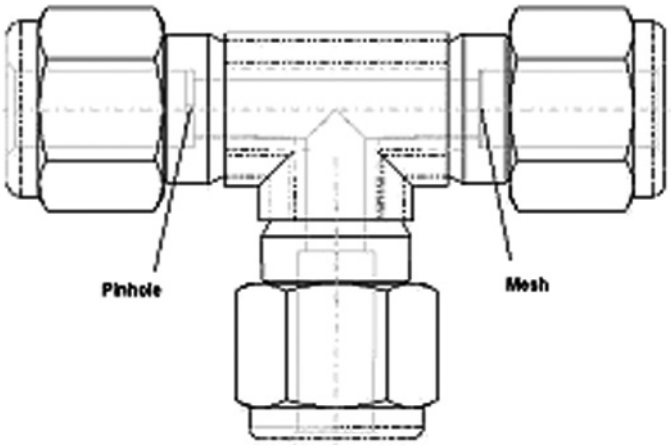

Fig. 3: injector of the turbulent mixer device. The liquid is injected from the left, thought the pinhole, the gas comes from the bottom port, and the foam is produced after the mesh.

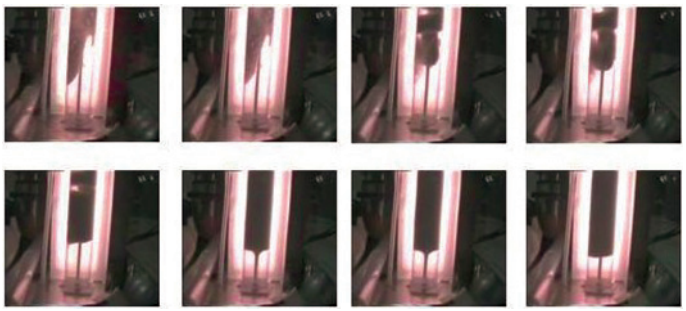

Fig. 4 : Filling of a cylindrical cell for foam analysis. The foam is injected form the bottom, where one can see the foam jet, and the foam accumulates at the top. The white illumination is from the back plane.

term stability issue (this surfactant molecule remains stable for months in solution). Depending on the tests, TTAB was used with or without the addition of a co-surfactant, dodecanol (DOH), which is known to stabilize foam and to rigidify the bubble interfacial layers.

Concerning foam production, we operated in microgravity six different devices, efficient on ground, in order to test if their use is similar in micro-g, and if they can still provide the required bubble size and liquid fractions. With such tests, we also obtained some knowledge on how foams behave in micro-g, and on which type of approach appears the most suitable for long term microgravity use.

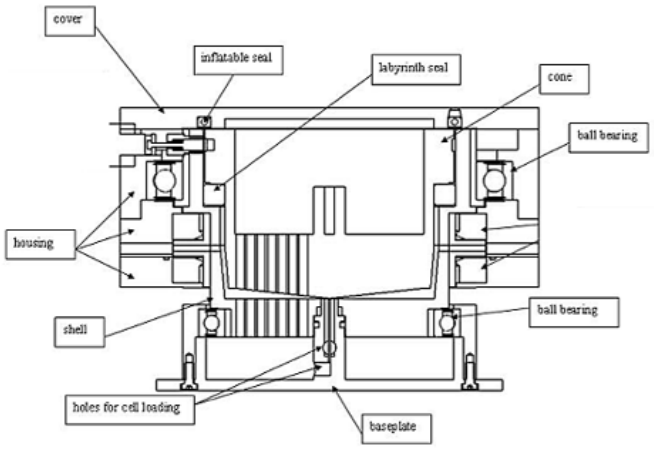

Fig. 5 : Drawing of one of the prototype cell investigated in the flights. The foam is restricted between the cone and the shell plate.

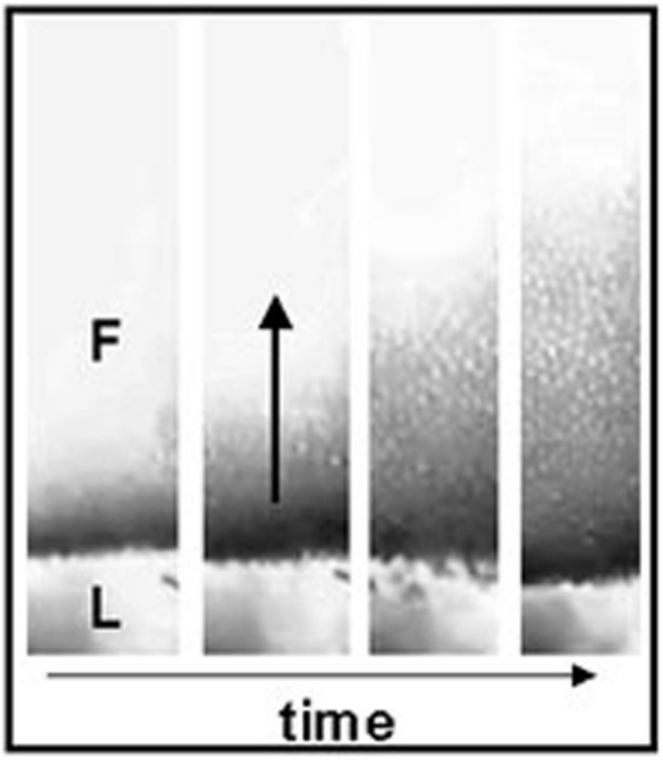

Fig. 6 : Foam pictures in transmission at different times during the microgravity conditions, evidencing the capillary imbibition into the foam (F) from the liquid reservoir (L).

Basically, to make an aqueous foam, one has to mix and incorporate a gas into a liquid which contains some surfactant molecules [1-3]. A first approach to make uniform and controlled foams is to use motorized mechanical mixer: gas and liquid are mixed inside a volume containing a quickly rotating moving part. In a first setup, the moving part is a metallic mesh which is rotating on the cell axis (drawing in Fig. 2a, and equipment at the right in Fig2b). The foam liquid fraction is controlled by the initial amount of gas and liquid in the cell. Once the foam is made, in typically in less than 30 s, it is pushed out of the mixer to the measurement cell by a piston, compressing the metallic grid. In a second setup, the moving part is a metallic spiral which is both rotating on the axis, and translating back and forth in the mixer. Fig. 2b shows a picture of this device (on the left). Tests in microgravity conditions showed that these devices work as efficiently as on the ground: small bubbles were produced, at different liquid fractions. However, they turned out to be rather fragile and very sensitive to vibrations, especially in relation with the long shaft axis. Indeed, slight deformations on this axis can either block the rotation or can induce leaks after many uses: both were observed during the flights. Moreover, the cleaning of such mixer cell may not be quite simple, and may requires large amounts of pure liquid.

A completely different method of foam production is known as the aerosol one (like in shaving cream can). The gas and the liquid surfactant solution are compressed in a closed vessel so that the gas gets into the liquid state. After mixing, one obtains an emulsion of the two liquids. Releasing the pressure at the outlet port nucleates some bubbles from the liquefied gas droplets. This technique is quite useful for making very small bubble sizes, and for high foam uniformity. In microgravity conditions, we tested a prototype (initially designed by NASA). Here again, though the fact that it proves its efficiency during the flights tests, this method has also its drawbacks. First, it is difficult to vary the liquid fraction in a simple and automatic manner with a single device: it has to be completely discharged, reloaded and compressed each time. Secondly, to avoid very high pressure for gas liquefaction, isobutane is used; but unfortunately, this gas appears not to be adapted to make stable foams.

A third approach consists of obtaining the mixing of gas and liquid as both fluids simply propagate together in tubes, and without moving parts for mixing. This can be done either with high pressure as in the turbulent mixer method [9]. In fig. 3, we show a drawing of the T-piece where the pressurized gas (under typically 5 bars) and the pressurized liquid (under typically 8 bars) meet. The liquid comes from the left and passes through a pinhole of diameter 0.5mm, while the gas comes from the perpendicular direction. After a first inserted mesh at the outlet port, a uniform foam with a low bubble size polydispersity is

created by the subsequent turbulent mixing obtained into a final hose of length 50cm and diameter 5mm, and without any variations of the foam properties during the steady-state production. We successfully tested that technique in the flight. Its main problems are here again linked to the module constraints: first, this device creates in a few seconds too large volume of foam (much more than what is needed); and secondly, before obtaining a good foam quality, a large foam volume of poor quality is produced and cannot be used, inducing complex problems of waste management. Also, the high pressure needed are not ideal for safety issues. In fact, similar simple mixing along tubes can be done though without high pressure, by creating a smooth circulation in a closed loop. The fluids motion is induced by a pump within the loop, and the mixing occurs slowly with time. Such a method has many advantages regarding the robustness with time, liquid recovery and minimal waste. However, it cannot be thoroughly tested on parabolic flights, as the foam formation usually takes more than a minute.

With all these generators, we studied the produced foam quality inside cylindrical transparent tubes of diameter 4cm. In figure 4, we show a sequence of pictures taken during a filling of such a transparent tube. The foam enters the tube from below, and appears dark as it is illuminated from the back [10]. Depending on the liquid fraction, the way the tube is filled differs: here, the foam liquid fraction is 12% and the foam rises up like a jet to the top, and eventually accumulates there, appearing as a rather solid pasty material.

During the three campaigns, we also tested different rheology-imbibition cell prototypes, allowing us to investigate some of the issues discussed in section 2. Figure 5 is a schematic of one of these prototype cells. The foam is injected from the bottom and is confined between the top cone and the bottom shell. Different types of sealing were tested: a contactless one based on a labyrinth design, and an inflatable one, allowing or not the sealing between the rotating cone and the housing. Observation for foam filling was done from above. The vertical lines on the left side of the cone and shell represent the electrical electrodes facing each other.

Note also that our tests confirmed that the addition of DOH to TTAB enhanced the foaming and foam stability as on ground, and no unexpected behavior were seen.

4. Imbibition Experiments

4.1 Liquid propagation in foams on ground and in micro-g

As said already, liquid and gas tend to separate on ground, inducing a liquid flow inside the foam. This flow is confined inside the network of interstitial liquid channels (the Plateau borders, PBs) which are located along the bubble edges, and with specific triangularlike cross section [1-6]. The gravitational drainage has been widely studied on ground, 9 evidencing different drainage regimes related to the bubble interfacial mobility [4-6]. The liquid flows between the bubble not only because of gravity but also because of capillarity, and the foam drainage results from a subtle balance between these two effects which can either transport the liquid in the same direction (like in the forced-drainage experiments where a wet foam is above a dry one) or in opposite direction (like in free-drainage where the wetter foam is below the dry one). The balance can be characterized by the Bond number μ, illustrating the ratio of gravitational forces over the capillary ones. The capillarity-induced liquid motion comes from liquid pressure differences due to variations of the local curvature of the PBs: capillarity tends to propagates liquid from a wet part of the foam (higher liquid

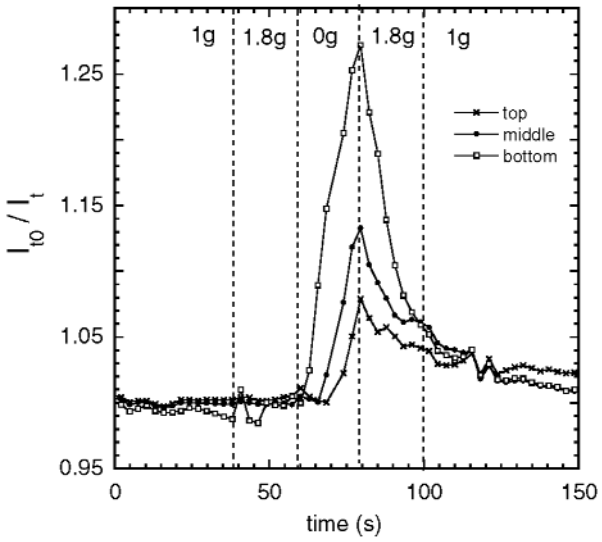

Fig. 7 : Time variation of the inverse of the transmitted intensity at three different positions during a parabola. The local liquid fractions follow the same behavior.

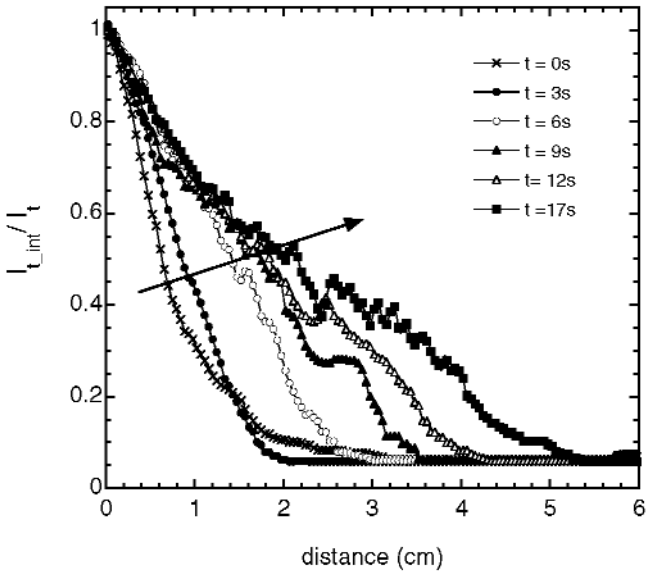

Fig. 8 : Vertical profiles of the inverse of the transmitted intensity (proportional to the liquid fraction) at different times (following the direction of the arrow). The triangles correspond to the initial state of equilibrium capillary profile.

pressure in the PBs) to a dry one (lower liquid pressure in the PBs), and thus also tends to eliminate gradients. Analysis of ground experiments (for instance, where the flow along two perpendicular dimensions is followed) can give some insights on the capillary contributions, though it remains always in a situation where the gravitational and capillary effects are coupled, at large B [11,12]. In fact, performing experiments in microgravity is the only way to study in a straightforward manner the details of the capillary contributions, at B << 1. Studying liquid propagation into a foam is in fact a way to scan its structure and geometry, and the balance between PBs, nodes and films. In that sense, such experiments in micro-g offer us an unique opportunity to better understand how the bubbles geometry and packing evolve as the liquid fraction is increased. It offers also the possibility to investigate liquid transport in already very wet foams, and should provide us some insights on the convective instabilities occurring in imbibition experiments on ground, when both gravity and capillarity are acting in the same direction [13,14]. In previous parabolic flights, preliminary experiments on capillarity-induced propagation have been done [15-17]. But these experiments only dealt with 2D foams (only one layer of bubbles between plates), which were moreover extremely polydisperse, and without any control of the physical chemistry, nor of the injection flow 10 parameters. On the theoretical side, this problem has been studied in details by Cox and Verbist in [18].

4.2 Experimental setup and technical details

We performed our imbibition experiments in a rectangular transparent cell (height H = 30cm, width W = 10cm and thickness T= 3cm). The foam is made during the normal gravity phase between parabolas by gently bubbling through the solution via a porous glass frit immerged at the bottom of the cell. The bubble diameter is about d = 3.2 mm, and the foam polydispersity is low. The evolution with time and position of the liquid fraction is followed by light transmission. As there are more than 10 bubbles in thickness, the light is multiply scattered as it passes through the foam: in that limit, the wetter the foam is, the darker it appears, as less light is transmitted [10,19]. The transmitted intensity It is thus inversely proportional to the liquid fraction, and this is the property that we are using in this work, but note that the exact quantitative relationship is not yet completely known [10, 19].

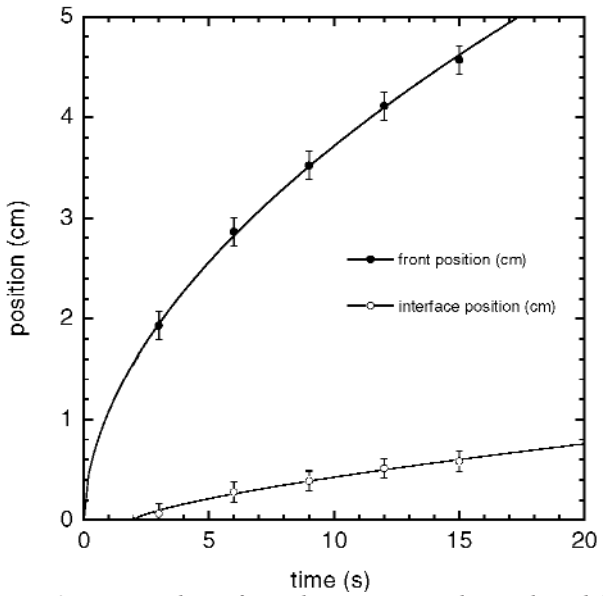

Fig. 9 : Front and interface relative positions during the imbibition experiment from a reservoir.

Experiments were done with a solution of TTAB+DOH for a few reasons. First, this provides more stable foams ; secondly, we are sure that the experiments should be well within the limit regime of low interfacial mobility [6] ; lastly, the predictions for the limit of low mobility indicate that the liquid propagation front is sharper (less extended in distance) than in the opposite case [18], thus being easier to detect. Indeed, the high surface mobility regime is more difficult to get at this bubble size: it requires very low surface viscosities, meaning extra pure and clean TTAB solutions without traces of DOH, and this was difficult to achieve with confidence within our flight setup.

During these experiments, the micro-gravity level is quite sufficient to get a low enough Bond number, so that capillary effects are significantly stronger than gravitational ones. The usual small fluctuations of micro-gravity level during the parabolas did not perturb 11 our measurements, and each measurements were performed many times to get enough statistics and to detect anomalous parabolas where the variations of gravity were too high.

4.3 imbibition from a liquid reservoir

The most simple imbibition experiment corresponds to a starting situation of a foam sitting on a liquid reservoir (same liquid as within the foam) under gravity. In this stage, the foam is almost completely drained, though it remains a small capillary hold-up just above the foam-liquid interface, resulting from the balance between gravity and capillary suction. At the interface, the liquid fraction ε rise up to 36%, which correspond to the random packing of undeformed solid spheres. Then, when the microgravity phase occurs, the gravity-capillarity equilibrium is broken, and one can investigate how the liquid irreversibly rises upward through the foam by capillarity (unidirectional propagation), while conserving always a foamliquid interface, and thus a fixed boundary condition at ε = 36%.

In figure 6, one can see pictures in transmission of the foam at thee times: the first one is the starting situation with the liquid hold-up at the interface just before the beginning of the micro-g conditions, the two others are during the micro-g phase ; the picture window is about 8cm in height and 3 cm in width. The capillary imbibition is clearly observed: the liquid rises into the foam, and the liquid fraction increases from the bottom, as the foam-liquid interface moves down. Note that on ground, in a drainage experiment, qualitatively similar pictures would have been found if one inverts the direction of time. One can then extract the transmission ratio I_0/I_t (I_0 is the initial transmitted

intensity of the dry foam, before the parabola) at three vertical heights (a first one being close to the cell bottom, another in the cell middle, and the third being close to the cell top) as a function of time, before, during and after a complete parabola (Fig. 7). The ratio shown here I_0/I_t follows the variation of the liquid fraction. During the micro-g phase, the liquid fraction rises at each position, with some time 12 delays indicating the times for the liquid to reach the successive positions. The rate of increase at each location is identical in agreement with the fact that the propagation is unidirectional. In the 1.8g resource phase of the end of the parabola, a strong decrease is seen due to the return of the downward gravity. The vertical profile of the normalized intensity are reported in Fig. 8. Here again I_{t_int}/I_t reflects the variation of the liquid fraction (I_{t_int} is the minimum transmitted light at the foam-liquid interface). Note also that the horizontal axis represents the distance from the interface. One can see that the foam is becoming more and more wet with time, and that capillarity tends to reduce the liquid vertical gradient. One can also see that there is a clear difference between the initial gravity-capillarity profile (white triangles) which is the result of the previous drainage before the beginning of the parabola and the imbibition liquid profiles under microgravity: in agreement with the predictions, at short times after the beginning of micro-g, the distance over which the liquid fraction varies from 1 to 0 is smaller than previously at equilibrium [18].

From all these measurements we can then study the time evolution of the position of the liquid front propagating into the foam, and of the foam-liquid interface (Fig. 9). The liquid front curve is determined by detecting at which time a change in transmission is detected at a given location. This procedure is similar to detecting, at a given time, the position at which the liquid profile crosses the horizontal baseline. Adjusting the front position by a power law At^{α} gives an exponent $\alpha = 0.48 +/- 0.03$. The error bars correspond to statistics over many measurements. This exponent is in complete agreement with the models (α is predicted to be 0.5, independently of the surface mobility [18]), evidencing the diffuse character of the propagation under micro-g. The prefactor A of such curve depends on the liquid fraction threshold ε_f at which the measured front is associated: for a given time, the higher ε_f, the smaller the liquid has propagated (as it can be understood in Fig. 8), thus the smaller prefactor. The prefactor also depends on the initial liquid fraction of the foam ε_0. Experimentally, ε_0 and ε_f are not zero. However, we know from previous forced-drainage experiments at this bubble sizes [6], that the initial foam liquid fraction is quite small ($\varepsilon_0 \approx 0.1\%$), and that we are able, with this technique of light transmission, to detect very low liquid fraction variations above this background, less than 0.5% and corresponding to the lowest forced flow rate. Thus, we believe that we should in fact be very close to the ideal situation of models where $\varepsilon_0 = 0$ and where the front is detected at εf slightly above 0. Indeed, from the calculations and in agreement with the simulations in [18], we find that our data points can be perfectly

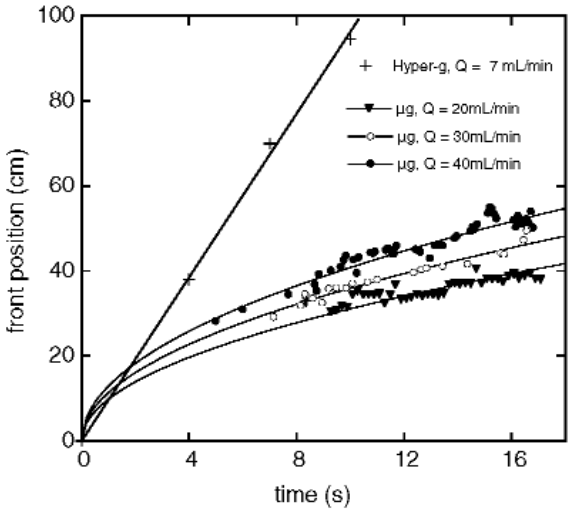

Fig. 10 : Foam pictures in transmission at three different times during the microgravity conditions, with liquid injection at the top (at a constant controlled flow rate).

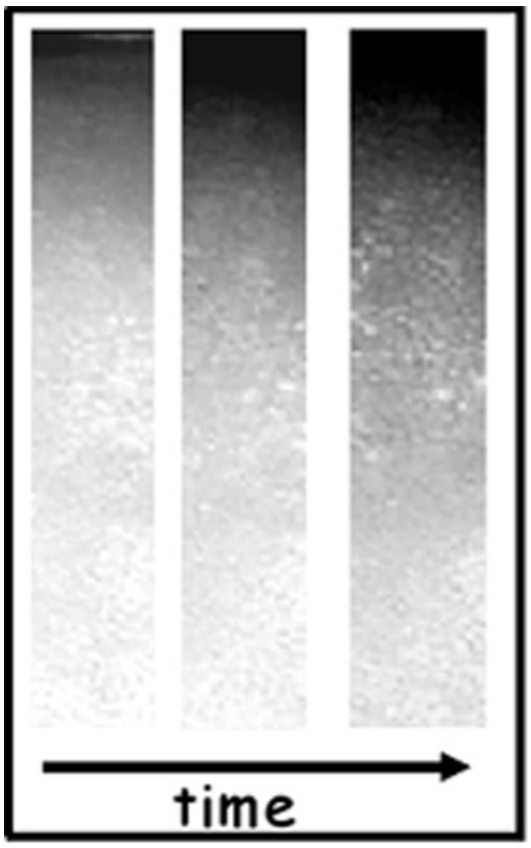

Fig. 11 : Front position as a function of time, at three different flow rates Q (20, 30 and 40mL/min) in microgravity conditions, and at a flow rate Q = 7 mL/min in hypergravity condition (crosses).

adjusted by the equations assuming low surface mobility, if one considers that we are experimentally detecting the front at ε_f = 0.3% (solid line through the points in Fig. 9). This is in agreement with what we expected, 0.1% < ε_f < 0.5%, meaning that also quantitatively we can provide a good analysis of these imbibition experiments. Such quantitative agreement validates the models developed in [18], as well as all the associated hypothesis, and geometrical constants used in it.

The variation of the position of the foam-liquid interface (measured positive when the interface moves downward) also follows a power law behavior in $t^{1/2}$. Note however that at short times, the interface does not move. Back to Fig. 6, one can see that at these short times, just after the beginning of the micro-g phase, there is a liquid redistribution from the previous capillary profile into the imbibition one: the liquid initially in this capillary profile is used to feed the imbibition one, thus there is no need for sucking more liquid out of the reservoir (and the interface thus remains still). At longer times, one can also comment on the ratio between the front position in the foam and the interface position. All the liquid which is spread inside the foam must be the one sucked from the pool, so this ratio can be seen as a mean liquid fraction in the whole foam. As the front rises about 7 times more than the interface moves, we finally find that this mean value is about 1/7= 15%: this is perfectly consistent with a liquid profile supposed to be almost linearly spread between 36% to 0% [18].

4.4 imbibition with constant input of liquid

In a more advanced experimental procedure, we studied the liquid propagation due to a constant input of solution, as in forced-drainage experiments on ground. During the micro-g phase, we have injected at the top of the cell and all along its width some liquid at a flow rate Q (from 5 to 50mL/min), resulting in a unidirectional situation of downward imbibition. Note that the cell is long enough so that such experiments at the top do not interfere with the capillary rise discussed before at the bottom. Figure 10 shows three pictures at different times after the injection, where it can be seen that some liquid is spreading into the foam. Note that due to our experimental setup, a shadow of the top part of the cell is always detected, preventing any measurements on almost the first 3 cm of the cell. With experiments using solutions of TTAB + DOH, front positions as a function of time for three different flow rates (20, 30 and 40 ml/min) are given in Fig. 11. Starting with the equations in [18] and adding the scaling with the flow rate Q, we find that in the limit of low surface mobility, the front position x_f follows $x_f = C\,K^{2/5}\,Q^{1/5}\,t^{3/5}$, where C is a constant (incorporating the bubble size, the solution viscosity and surface tension, geometrical constants, and the cell section - in these experiments, C = 0.85), K is the foam permeability, Q the flow rate and t the time. Experimentally, the $x_f(t)$ curves can be adjusted by power law functions of the type $A\,t^{\alpha}$, and we find that α = 0.48 +/- 0.05 (Fig. 11). This exponent turns out to be very close, though slightly below the predicted one (3/5). Note however that the range of position variation is small, and that the short times are not accessible: this makes difficult a very accurate estimation of this exponent, needed for possibly claiming the existence of a significant difference with the model. It is also possible that at this small distance from the injection, a completely unidirectional flow may not yet be completely established. More measurements are foreseen in different geometries to better test the scaling with time. Nevertheless, one can 15 also test the dependence with the flow rate Q. As seen in Fig. 11, the dependence is small, and experimentally we find that, when forcing the exponent α to the predicted value 3/5, the resulting prefactor A can itself also be fitted by a power law curve BQ^{β}, , with B = 0.133 and β = 0.22. This new exponent β appears in good agreement with the predictions (1/5), and from the prefactor B we can finally extract the foam permeability K, $K= (B/C)^{5/2} = 9.7\ 10^{-3}$ (representing, in this low mobility limit, the permeability of the PB network). This value is slightly above the theoretical value, $K = 6.6\ 10^{-3}$, for an infinitely small mobility M [4]. In fact, knowing the relationship, K(M), between K and the surface mobility M [6], we find that it corresponds to a finite mobility parameter M ≈ 0.15 (M depends on the bubble size, liquid fraction, surface and bulk viscosities). This result confirms first that our experiments indeed fall into the low mobility regime, when M < 1, and secondly a value of M ≈ 0.15 is exactly what can be expected for these experimental conditions [6]. Thus, as for the previous results on imbibition from the liquid reservoir, these first experiments of imbibition at controlled flow rate under microgravity are both qualitatively and quantitatively in agreement with the models, which appear to successfully describe the capillarity-induced propagation of liquid into a foam (especially the liquid front features). However, more quantitative experiments (based on electrical conductivity) are foreseen to continue to tests other imbibition features, at different surface mobility and at higher liquid fractions.

Lastly, we also took advantage of the hypergravity phases obtained during the parabolic flights, and performed the same controlled imbibition experiments at an acceleration of 1.8g. In Fig. 11, the front position measured for such an experiment at Q=7 mL/min is shown. As on ground, the liquid front moves linearly down into the foam, and the slope is found to be about twice bigger than what is known in normal gravity, in agreement with the classical drainage equations.

5. Conclusions

The FOAM module for the ISS is a complex but exciting project, as it deals with many different topics (optics, mechanics, hydrodynamics, electronics, physical chemistry) studied under microgravity conditions. Many results on aqueous foams under microgravity conditions have been collected during the parabolic flights campaigns, both on technical issues and on the scientific ones, showing how useful such short duration microgravity conditions in parabolic flights can already be. Tests on foam production have shown that it is possible to make stable

foams of controlled properties under microgravity conditions. Though the use and the outputs of the methods tested do not often differ from what is found on ground, a main result here relates more on the reliability of the method itself, and its adaptation to the microgravity conditions and ISS requirements. On the scientific side, we have reported here the first imbibition experiments on 3D foams, with controlled bubble size, chemical interfacial properties, and injection rate. So far, the analysis of such results are in close agreement with the theoretical predictions. Such results have also an impact on the future long time experiments in the ISS, as it help us to continuously optimize the experimental schedule and procedure.

Acknowledgements

The authors want to thank T. Hummel , P. Wikus, and J. Winter from EADS-ST for technical support, and for providing some of the drawings. We also thank S.J. Cox and D.J. Durian for discussions, J. Dubail from Ecole Polytechnique for help in calculations and simulations, and ESA for financial support through the MAP program. 17

References

[1] *R. K. Prud'homme and S.A. Khan,* Foams, Theory, Measurements, and Applications, Surfactant Science series, New York, Marcel Dekker Inc. , Vol. 57 (1997).
[2] *Weaire D. and Hutzler S.,* The Physics of Foams, Oxford University Press, 1999.
[3] *A. Saint-Jalmes, D.J. Durian, D.A. Weitz,* Foams, Kirk-Othmer Encyclopaedia of Chemical Technology , vol. 11, 5th edition (2004). Edited by Wiley InterScience.
[4] *Cox S., D. Weaire, S. Hutzler, J. Murphy, R. Phelan and G. Verbist,* Proc. R. Soc. Lond. A, 456, 2441, 2000.
[5] *Koehler S. A. , Hilgenfeldt S. and Stone H. A.,* Langmuir, 16, 6327, 2000.
[6] *Saint-Jalmes A. Zhang Y. and Langevin D.,* Eur. Phys. J. E, 15, 53, 2004.
[7] *H. A. Barnes, J. F. Hutton and K. Walters.* An Introduction to Rheology, Amsterdam: Elsevier. 1989.
[8] *A.D. Gopal and D.J. Durian,* J. Coll. Int. Sci., 213, 169, 1999.
[9] *A. Saint-Jalmes, M.U. Vera, D.J. Durian,* Eur. Phys. J. B, 12, 67, 1999.
[10] *M.U Vera, A. Saint-Jalmes and D.J Durian,* Applied Optics 40, 4210, 2001.
[11] *S.A. Koehler, S. Hilgenfeldt and H.A. Stone,* Europhys. Lett. 54 (3), 335, 2000.
[12] *S. Hutlzer, S.J. Cox, G. Wang,* Colloids and Surface A, 263, 178, 2005.
[13] *S. Hutzler, D. Weaire and R. Crawford,* Europhys. Lett. 41 (4), 461, 1998.
[14] *M.U. Vera, A. Saint-Jalmes and D.J. Durian,* Phys. Rev. Lett. 84 (13), 3001, 2001.
[15] *Noever D. and Cronise R.,* Phys. Fluids, 6, 2493, 1994.
[16] *H. Caps, H. Decauwer, M.-L. Chevalier, G. Soyez, M. Ausloos, and N.Vandewalle,* Eur. Phys. J. B 33, 115, 2003 ; H. Caps, S.J. Cox, H. Decauwer, D. Weaire, N. Vandewalle, Colloids Surfaces A, 261, 131, 2005.
[17] *S.J. Cox, D.W. Weaire, G. Verbist,* Eur. Phys. J. B, 40, 119, 2004.
[18] *Cox S. and Verbist G.,* Microgravity Sci. Technol., 14, 45, 2003.
[19] *A.S. Gittings, R. Bandyopadhay, D.J. Durian,* Europhys. Lett. 65(3), 414, 2004.